Characterization of Organosolv Lignins using Thermal and FT-IR Spectroscopic Analysis

Rhea J. Sammons,[a] David P. Harper,*[,b] Nicole Labbé,[b] Joseph J. Bozell,[b] Thomas Elder,[c] and Timothy G. Rials [b]

A group of biomass-derived lignins isolated using organosolv fractionation was characterized by FT-IR spectral and thermal property analysis coupled with multivariate analysis. The principal component analysis indicated that there were significant variations between the hardwood, softwood, and grass lignins due to the differences in syringyl and guaiacyl units as well as the different processing temperatures and times used to isolate the lignins. Partial least squares regression revealed that the concentration of syringyl units was the foremost factor behind the variation in glass transition temperature (T_g) for each lignin sample. It was concluded that structural variations resulting from altering the processing time and temperature and the lignin species directly affect the thermal properties of the lignin. Therefore, by determining the thermal properties of a lignin sample, a basic understanding of its structure can be developed.

Keywords: Lignin; FT-IR; DSC analysis; Organosolv; Multivariate analysis; Glass transition

Contact information: a: Archer Daniels Midland Company, Decatur, IL 62526 USA; b: Center for Renewable Carbon, The University of Tennessee, 2506 Jacob Dr, Knoxville, TN 37996-4570 USA; c: USDA-Forest Service, Southern Research Station, 2500 Shreveport Highway, LA 71360;
** Corresponding author: dharper4@utk.edu*

INTRODUCTION

Lignin has traditionally been viewed as a low-valued waste byproduct of the pulp and paper industry (Stewart 2008). As determined in previous lignin studies, the processing conditions used to produce paper, mainly sulfite and kraft, cause the lignin fraction to have a high amount of impurities that limit the use of lignin in other applications that require a "clean" lignin (Lora and Glasser 2002). This limitation significantly decreases lignin's suitability as a resource for future processing, and as a result, only 1 to 2% of traditionally processed lignin is used for products other than fuel sources for process heat (Hamelinck *et al.* 2005).

In the United States, forest biomass is consumed at a rate of 129 million dry tons annually and has the potential to grow to a size 2.5 times its current use on a sustainable basis (U.S. Department of Energy 2011). A large research effort has targeted the conversion of all the fermentable sugars in lignocellulosic biomass into fuel ethanol. There are many obstacles to overcome before this will be economically feasible. However, if a fraction of the 368 million dry tons available is converted into liquid fuels, a large amount of extracted lignin will be produced as a byproduct. Lignin resides in grasses, shrubs, and trees as a network polymer that is largely non-hydrolysable. Lignin physically protects polysaccharides from extraction and must be disrupted in order for enzymes to gain access (Kirk and Chang 1981). Many processes are available and are

used in the extraction of lignin for paper and other products. Each of these processes yields lignin with varying purity and chemical characteristics depending on the extraction process and feedstock. Regardless of the source of the lignin byproduct, an essential component of the viability of a biorefinery must be the successful utilization of lignin in new materials and chemicals in order to add value to the process as a whole.

The structural variations in lignin due to the processing conditions are challenges that are starting to be overcome so that lignin may be used in a multitude of applications. A variety of lignin preparations with different chemical structures and physical properties, depending on the feedstock and the pretreatment used in the refining process, can be generated and utilized in new applications such as bioplastics and fibers. However, understanding the differences as well as the similarities within this new group of lignins is vital in determining how these lignins can be fully converted into new products. The characterization of a small test group of alternative lignins by Fourier transform infrared (FT-IR) spectroscopy and differential scanning calorimetry (DSC) was undertaken to establish a foundation for more extensive study of the structure-property relationships of lignin.

EXPERIMENTAL

Materials

The lignins used for this study were obtained from a range of hardwoods, softwoods, and crop residues that were prepared *via* organosolv technology with alterations in the processing method. The lignins used for this statistical analysis were chosen from a sample set that were processed under the varied conditions listed in Table 1. The solvent-based fractionation uses a mixture of organic solvents and water in the presence of an acid catalyst to cleanly separate the cellulose, hemicellulose, and lignin in biomass (Bozell *et al.* 2011a). As a result of this fractionation, the purity of the cellulose is increased and the resulting lignin and hemicellulose can be used as feedstocks for higher value products compared to the conventional technologies that use lignin as fuel. Two commercial lignins, Alcell (organosolv process) and Indulin AT (kraft process), were also analyzed for comparison.

Processing Conditions

The processing conditions selected to obtain the lignin samples represent the types of fractionations being tested in order to represent possible conditions in an organosolv biorefinery. Table 1 indicates the processing parameters that were varied during the lignin preparation, where the temperature is in degrees C, the time is in minutes, and the amount of the catalyst in the process, H_2SO_4, is in moles/liter. The methyl isobutyl ketone (MIBK) level specifies the amount of MIBK used in the process in relation to the amount of ethanol and water, whereas the ratio listed in the table is MIBK to ethanol to water. These processing conditions resulted in a varied pulp and lignin yield. Samples that do not have processing conditions listed were commercial lignins.

Thermal analysis was performed using a Q1000 differential scanning calorimeter from TA Instruments. Approximately 4 mg of each lignin sample was placed in a hermetically sealed DSC pan. The top of each sealed pan was punctured to allow

volatiles to escape. Samples were equilibrated at 0 ºC, heated at a rate of 10 ºC/min to 200 ºC, cooled to 0 ºC at 10 ºC/min, and again heated to 200 ºC at a rate of 10 ºC/min. All samples were tested in triplicate. The glass transition temperature (T_g) was determined at the midpoint temperature of the heat capacity change for the second heating run.

Table 1. Processing Parameters

Lignin	Temp (°C)	Time (min)	Amt of H_2SO_4 used (M)	MIBK/ EtOH/ Water Level (%)	Lignin	Temp (°C)	Time (min)	Amt of H_2SO_4 used (M)	MIBK/EtOH/ Water Level (%)
Alcell*	---	---	---	---	Mixed Hardwoods	120	240	0.15	16/34/50
Pine*	200	32	0.1	16/34/50	Mixed Hardwoods	130	240	0.15	16/34/50
Bagasse*	120	56	0.1	16/34/50	Mixed Hardwoods	130	180	0.175	16/34/50
Eucalyptus*	140	56	0.1	16/34/50	Mixed Hardwoods	125	225	0.19	16/34/50
Aspen	140	56	0.2	16/34/50	Mixed Hardwoods	125	225	0.19	16/34/50
Aspen*	140	56	0.2	16/34/50	Mixed Hardwoods	125	225	0.19	16/34/50
Mixed Oak*	140	56	0.05	16/34/50	Mixed Hardwoods	125	225	0.19	16/34/50
Tulip Poplar*	140	56	0.075	16/34/50	Mixed Hardwoods	125	225	0.19	16/34/50
Tulip Poplar*	140	56	0.175	16/34/50	Mixed Hardwoods	125	225	0.19	16/34/50
Tulip Poplar	160	56	0.1	16/34/50	Switchgrass*	140	54	0.1	44/32/24
Mixed Oak*	140	56	0.175	16/34/50	Black Locust*	140	56	0.1	16/34/50
Mixed Hardwoods*	140	56	0.175	16/34/50	Corn Stover*	140	56	0.1	44/32/24
Mixed Hardwoods	140	240	0.15	16/34/50	Newsprint*	140	56	0.1	44/32/24
Mixed Hardwoods	130	180	0.175	16/34/50	Indulin*	---	---	---	---
Mixed Hardwoods	125	120	0.15	16/34/50					

Note: (*) indicates the samples used in the PCA.

FT-IR Spectral Analysis

Spectra were collected using a Thermo-Nicolet Nexus 670 FTIR with a Golden Gate MKII single reflection ATR system. Spectra were recorded in absorbance mode from 4000 to 650 cm^{-1} at 2 cm^{-1} resolution with 32 scans per spectrum. Five spectra were collected for each lignin sample, and background spectra were collected in air.

A Principal Component Analysis (PCA) and Partial Least Squares regression (PLS) analysis of the FTIR data was performed using Unscrambler 9.0 developed by CAMO Software Inc. Before analysis, the spectral resolution was reduced from 2 to 4 cm^{-1}. The spectra were then normalized and full multiplicative scatter correction (MSC) was applied. Following the data pretreatment, the first PCA was carried out on 15 lignin samples selected from the 32 initial samples representing the lignin species, all with similar processing conditions. The second PCA was conducted on the 13 mixed hardwood samples that all had varied processing parameters.

The PLS regression was performed between the spectral data and the T_g data obtained from the DSC analysis on all 32 samples. The number of principal components (PCs) was determined based on the reaction of the residual response variance. When additional PCs did not decrease the residual response variance significantly, the model was completed. The PLS regression coefficient plot was used to determine the chemical and structural features of the lignin samples that drove the calibration and thus impacted the glass transition temperature.

RESULTS AND DISCUSSION

DSC Analysis

The results of the DSC analysis are summarized in Table 2. The table includes the glass transition temperature (T_g) and the change in the heat capacity (ΔC_p) for all the lignin samples. The table indicates that the lowest ΔC_p for the samples was obtained for a mixed hardwood at 0.009, and that the highest was obtained for pine at 0.417 J/g^{o}C. The lowest T_g was obtained for the aspen lignin at 89.9^{o}C. The highest T_g was from a mixed hardwood lignin at 180.6 ^{o}C. This temperature range is consistent with findings that un-derivatized lignin can have a temperature range between 90 and 180^{o}C (Feldman *et al.* 2001; Glasser and Jain 1993). With regard to preparation methods, kraft lignins have higher T_g values, whereas organosolv lignins have lower values (Tejado *et al.* 2007). In addition to the heat capacity, the processing parameters can also affect the T_g values, as illustrated by the varied range of temperatures for the mixed hardwoods. The variations in T_g values for the selected lignins as well as the variations in heat capacity illustrate the variations in their chemical structures, which can be correlated to the variations in the flexibility of the polymeric chains, the degree of crosslinking, and the amount of impurities (Khan and Ashraf 2007; Kubo and Kadla 2004).

Table 2. Averaged DSC Results

#	Lignin Type	T_g (^{o}C)	DC_p (J/g	#	Lignin Type	T_g (^{o}C)	DC_p (J/g
1	Alcell*	108.	0.403	18	Mixed	109.	0.141
2	Pine*	107.	0.417	19	Mixed	134.	0.064
3	Bagasse*	116.	0.386	20	Mixed	173.	0.034
4	Eucalyptus*	136.	0.182	21	Mixed	165.	0.063
5	Aspen	162.	0.102	22	Mixed	176.	0.055
6	Aspen*	89.9	0.230	23	Mixed	161.	0.043
7	Mixed Oak*	174.	0.141	24	Mixed	168.	0.025
9	Tulip Poplar*	119.	0.315	25	Mixed	162.	0.062
10	Tulip Poplar*	127.	0.206	26	Switchgrass*	121.	0.239
11	Tulip Poplar	141.	0.078	27	Black Locust*	105.	0.248
12	Mixed Oak*	96.9	0.282	28	Corn Stover*	131.	0.060
13	Mixed	100.	0.155	29	Newsprint*	140.	0.105
14	Mixed	180.	0.034	30	Indulin AT*	151.	0.123
15	Mixed	162.	0.117	31	Mixed Oak*	106.	0.250
16	Mixed	144.	0.009	32	Mixed	172.	0.043
17	Mixed	163.	0.029				

Note: (*) indicates the samples used in the PCA.

FT-IR Spectra Analysis

The averaged FT-IR spectra for a group of lignins in the range 2000 to 800 cm^{-1} are shown in Fig. 1 with peaks labeled. The assignment of the observed key peaks representing lignin structure is summarized in Table 3 and compared to published peak ranges from four sources (Faix 1991; Schultz and Glasser 1986; Popescu *et al.* 2007; Tejado *et al.* 2007). The band appearing at 1205 cm^{-1} was not consistent with an expected lignin spectrum, indicating that material other than lignin was present in the sample. This band could represent OH in-plane bending in carbohydrates and may indicate residual sugars (Popescu *et al.* 2007).

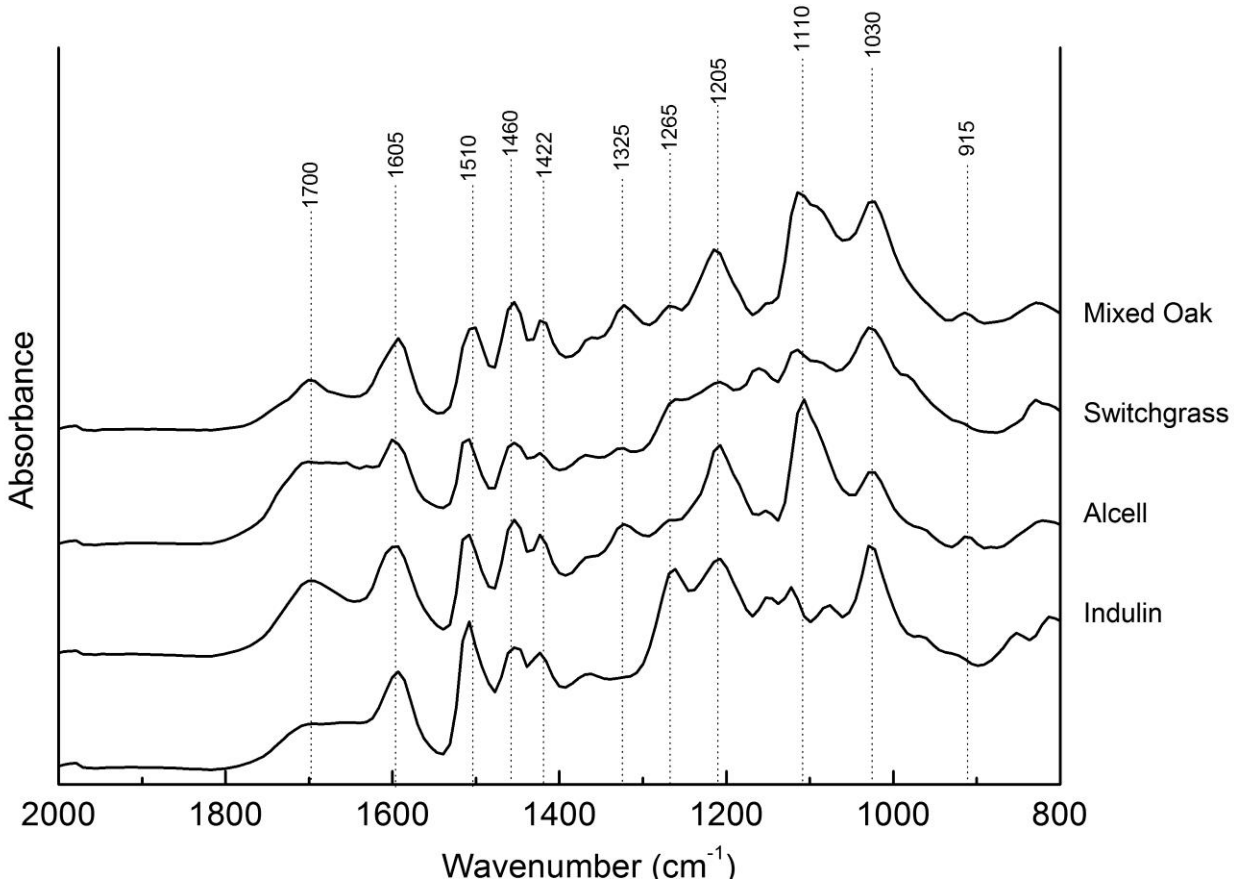

Fig. 1. FT-IR spectra for selected lignin types

Table 3 represents the wavenumber range for the bands observed in the lignin spectra and indicates lignin types based on the structural units present. Lignins with only guaiacyl rings are referred to as G units, lignins with both guaiacyl and syringyl rings are GS units, and lignins with small amounts of p-hydroxyphenyl units are classified as HGS.

Syringyl to Guaiacyl Ratio (S/G Ratio)

The comparison of the S and G structural units of lignin using the FT-IR spectra is one indication of the key differences among the lignin sources. Table 4 compares the S/G ratios determined from the magnitude of the deconvoluted peaks at ~1325 and ~1268 cm^{-1} for all the lignin samples (Faix 1991). The peak at ~1325 cm^{-1} resulted from the C-O stretching of the S ring, and the peak at ~1265 cm^{-1} resulted from the C-O stretching of the G ring (Faix 1991).

The hardwood lignins have more S units than do softwoods and grass lignins as indicated in Table 4 by the higher S/G ratios. The softwood and grass lignins have lower S/G ratios. In the paper industry, higher S/G ratios are important and indicate high delignification rates by alkali processes, which lead to a higher pulp yield (Margues *et al.* 2008). As shown in Table 4, hardwoods have a higher S to G ratio in comparison to the softwood and grass lignins, and this results from a greater concentration of S ring units.

Table 3. Assignments of Lignin IR Bands

Observed bands (cm^{-1})	Band assignment	A	B		C	D
			G unit	GS units		
1708	Non-conjugated carbonyl	1738-1709	1715	1715-1710	1740-1720	1705-1715
1655	Conjugated carbonyl	1675-1655	1675-1660	1660	---	1650
1605	Aromatic ring	1605-1593	1605	1595	1610-1595	1600
1510	Aromatic ring	1515-1505	1515-1510	1505	1515-1505	1515
1460	C-H deformation methyl and methylene	1470-1460	1470-1460		1470-1455	1460
1425	Aromatic ring stretching with in plane C-H deformation	1430-1422	1430	1425	1430-1425	1425
1325	C-O stretch of S ring	1330-1325	---	1330-1325	1335-1320	1326
1265	C-O stretch of G ring	1270-1266	1270	1275	1268	1270
1221	C-C, C-O, C=O stretch in G ring	1230-1221	1230	---	---	1220
1166	C=O stretch in ester group of HGS lignin	1166	---	---	1162-1125	---
1140	C-H stretch in G ring	1140	1140	1145	1140	---
	Aromatic C-H deformation of G units	---	---	---	---	1125
1110	Aromatic C-H deformation of S units	---	---	---	1128-1110	1115
1086	C-O stretch of secondary alcohols and aliphatic ethers	1086	1085	1085	1086-1075	---
1030	C-O, primary alcohols	1035-1030	1035	1030	1060-1015	1030
984	-CH=CH- bending	990-966	---	---	970	
915	Aromatic ring	925-915	855-815	915-860	930-915	
	C-H bending of G units	---	---	---	---	855
829	C-H bending of S units	832-817	---	---	---	825

A: (Faix 1991), B: (Schultz and Glasser 1986), C: (Popescu *et al.* 2007), D: (Tejado *et al.* 2007).

Table 4. S/G Ratios for Selected Lignin Types

Lignin Type	1325/1268 cm^{-1}	Lignin Type	1325/1268 cm^{-1}
Alcell	4.30	Mixed Oak 2	2.95
Pine	0.053	Mixed hardwoods	2.60
Bagasse	1.12	Switchgrass	0.433
Eucalyptus	4.25	Black locust	0.902
Aspen	1.51	Corn stover	0.483
Mixed Oak 1	2.60	Newsprint	0.033
Tulip poplar 1	5.23	Indulin AT	0.011
Tulip poplar 2	4.28		

PCA of FT-IR Spectra for Selected Lignin Types

PCA was carried out on 75 pretreated spectra (15 samples and 5 replicates). PCA is a statistical method that visually represents the differences in a data set (Martens and Naes 1989; Geladi 2003). PCA removes redundancy in the data set, converting it into a low number of loadings. These loadings include the majority of the important spectral information and retain most of the original spectral content. Each sample is scored on each principal component (PC), which reflects the sample location along the PC. The plotting of the PC scores against one another can reveal cluster patterns in the data set, which group together samples with similar chemical compositions (Martens and Naes 1989). Based on the residual variance curve, 4 was the optimal number of PCs, with PC1 accounting for 59% and PC2 for 18% of the total variance. The scores plot for the PC1 versus PC2 is shown in Fig. 2A. Three distinct clusters can be observed along the PC1 and PC2 axis. Along the PC1 axis, the right side of the plot shows the cluster of hardwood lignins, and the left side depicts the softwood and grass lignins. Along the PC2 axis, the upper cluster represents the grass lignins and the lower cluster represents the softwood lignins. This indicates that there are distinct structural differences between the three groups of lignins. The loadings plots further illustrate the key structures responsible for the variation between the groups. Beyond the variation in species, the differences may be explained by the delignification process and the varying process conditions used (Table 1). The dominant chemical process during fractionation is the cleaving of polysaccharides from lignin under mild conditions (Bozell *et al.* 2011b). In ethanol organosolv processes, the cleavage of α-aryl ether bonds appears to be rate-limiting (El Hage *et al.* 2010). As temperatures and acid concentration increases, additional disruption and solvolysis of the lignin structure occurs. The condensation of aromatic components and the electrophilic introduction of ethyl groups are also possible under severe reaction conditions (Bozell *et al.* 2011b; El Hage *et al.* 2010). The relative amounts of reaction product are dependent on composition, which itself is species-dependent.

Figure 2B depicts key differences in structure between the hardwood, softwood, and grass lignins. These peaks, as stated in Table 3, are as follows: 1655 cm^{-1}, the conjugated carbonyl; 1505 cm^{-1}, the aromatic ring of GS lignin; 1460 cm^{-1}, the C-H stretching of the methyl and methylene; 1325 and 1266 cm^{-1}, the S and G units, respectively, of ring stretching; 1140 cm^{-1}, the aromatic C-H in-plane deformation; 1086 cm^{-1}, the C-O deformation in the secondary alcohols and aliphatic ethers; and 906 cm^{-1}, the aromatic ring of GS lignin (Faix 1991; Schultz and Glasser 1986; Popescu *et al.* 2007).

These variations are the presence of the S ring units at 1325 cm^{-1}, the presence of the G ring units at 1266 cm^{-1}, and the C-H bending of the G ring units at 1140 cm^{-1}. The largest difference in the lignins resulted from the presence of secondary alcohols and aliphatic ethers indicated by the 1086 cm^{-1} peak (Faix 1991; Schultz and Glasser 1986; Popescu *et al.* 2007). This indicates that the concentrations of G and S rings as well as the presence of alcohols and ethers are the key differences that separate hardwood lignins from other species of lignins. The strong peak at 1086 cm^{-1} is indicative of the differences in carbohydrate content between the hardwoods and the grasses and softwoods. A recent study has indicated that residual sugars exist in switchgrass lignin (Bozell *et al.* 2011b) and that very low concentrations of carbohydrates are present in hardwoods (Bozell *et al.* 2011a) after pulping under similar conditions as used here. Some differences can also be observed among the softwoods, most likely from the pulping process: kraft for Indulin, organosolv for (recycled) newsprint, and organosolv for pine.

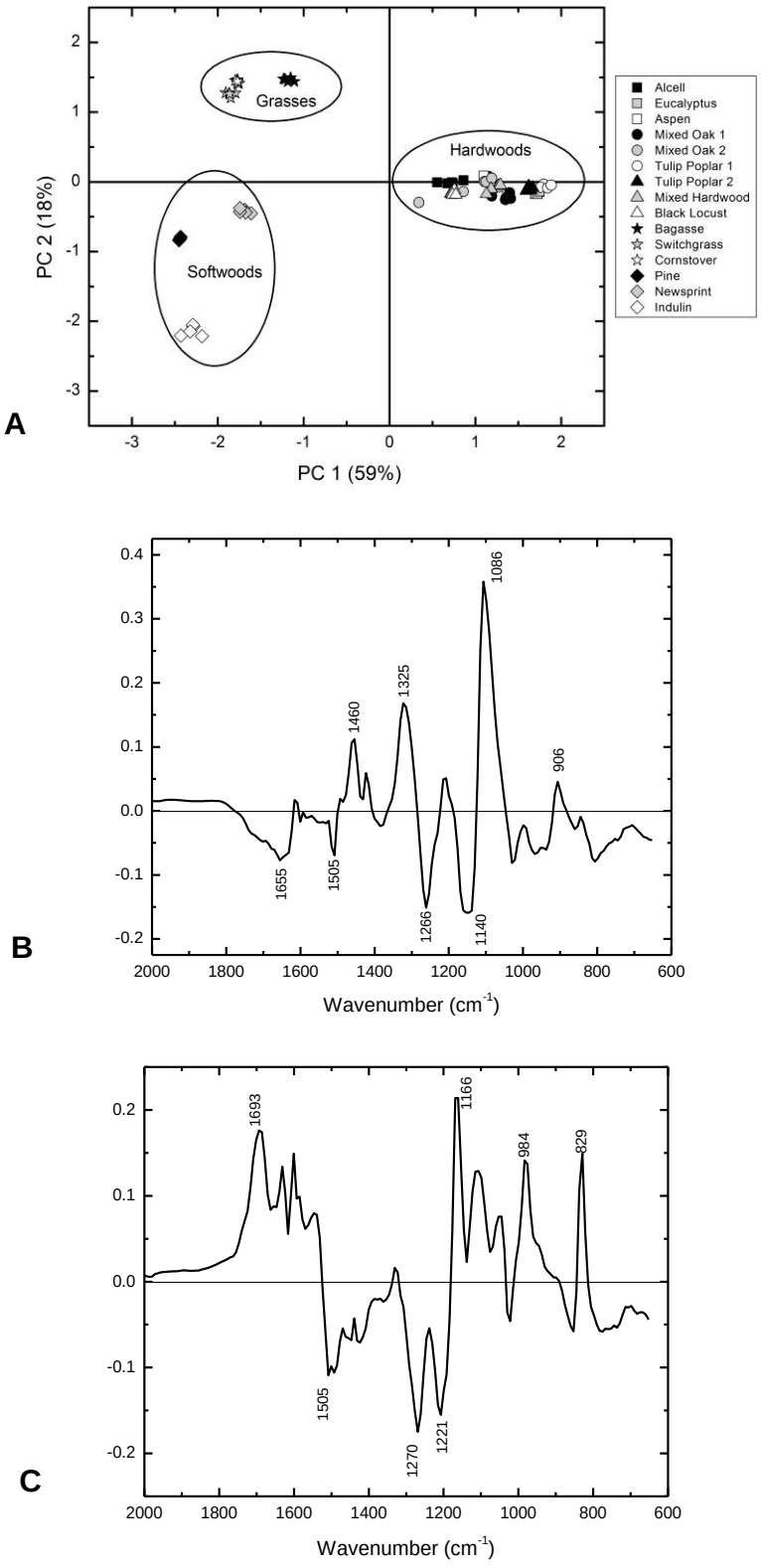

Fig. 2. (A) Scores plot for the PC1 and PC2 for selected lignin types, (B) loadings of PC1, and (C) loadings of PC2

Figure 2C represents the loadings for PC2 and is an indicator of the important structural variations between the wood and grass lignins. These peaks, as stated in Table 3, are as follows: 1708 cm^{-1}, the non-conjugated carbonyl; 1505 cm^{-1}, the aromatic ring of GS lignin; 1270 cm^{-1}, the C-O stretch of G ring; 1221 cm^{-1}, the C-C, C-O, C=O stretch in G ring; 1166 cm^{-1}, the C=O stretch in the ester group of HGS lignin; 984 cm^{-1}, the -CH=CH out-of-plane deformation; and 829 cm^{-1}, the C-H out-of plane deformation of the G unit 2,3 and 6 positions (Faix 1991; Schultz and Glasser 1986; Popescu *et al.* 2007). There are weaker bands indicating more differences in the lignin structure and carbohydrate content between wood and grasses at 1600 cm^{-1} (aromatic stretching) and at 1100 cm^{-1} (ether stretching).

The peak at 1166 cm^{-1} indicates that the primary difference in chemical structure between the commercial Indulin AT lignin and the grass feedstock lignin is the presence of ester groups. The other key variations are noticeable in the G ring unit at 1505 and 1270 cm^{-1}. As expected, this indicates that the concentration of G rings is the most significant difference between softwood and grass lignins. Another observation is the location of the Indulin AT commercial lignin in relation to the other softwood organosolv lignins shown in Fig. 2. Since the Indulin AT lignin possesses a more negative score along PC2 compared to the pine and newsprint lignins, this could indicate that the commercial processing conditions caused variations in the chemical structure in addition to those variations related to the differences in lignin species type.

The scores plot for the PC1 versus PC2 for only the hardwoods is shown in Fig. 3A. Most of the samples are distinct from each other along the PC1 and PC2 axis with the exception of the two tulip poplar samples, which are clustered together. The eucalyptus lignin is close to the tulip poplar, indicating similar chemical structures for the two types. The aspen and black locust lignins are also close along the PC1 axis, also indicating that the structural differences between them are minimal. The loadings plots further illuminate the key structures responsible for the variations between the groups.

Figure 3B represents the loadings plot for PC1, indicating the structural features responsible for the separations of the samples shown in Fig. 3A. The peaks in Fig. 3B represent the differences in structure between various hardwood lignins. These peaks, as stated in Table 3, are as follows: 1605 cm^{-1}, the aromatic ring stretching of the G ring; 1515 and 1505 cm^{-1}, the stretching of the aromatic rings; 1325 cm^{-1}, the C-O stretching of S ring; 1166 cm^{-1}, the C=O stretching in the ester group of HGS lignin; 1122 cm^{-1}, the C-O stretching; and 1030 cm^{-1}, the C-O deformation in the primary alcohols. The weak peak at 1415 cm^{-1} is not from lignin spectra but rather is caused by the carboxyl groups of polysaccharides (Faix 1991; Schultz and Glasser 1986; Popescu *et al.* 2007).

The largest bands in Figure 3B represent the major structural differences along the PC1 axis. The key structural differences come from the ester groups of the HGS lignin at 1166 cm^{-1} and the primary alcohol groups at 1030 cm^{-1}. This indicates that the largest differences between the mixed oak lignin and the commercial Alcell lignin are due to carbonyl, ester, and alcohol groups.

Figure 3C represents the loadings plot for PC2. These main peaks are 1724 cm^{-1}, the non-conjugated carbonyl; 1460 cm^{-1}, the C-H stretching of the methyl and methylene; 1325 cm^{-1}, the C-O stretching of S rings; 1265 cm^{-1}, the C-O stretching of G rings; 1140 cm^{-1}, the aromatic C-H in-plane deformation; 1110 cm^{-1}, the aromatic C-H deformation of S units; 1030 cm^{-1}, the C-O deformation in the primary alcohols; and 906 cm^{-1}, the aromatic ring of GS lignin (Faix 1991; Schultz and Glasser 1986; Popescu *et al.* 2007).

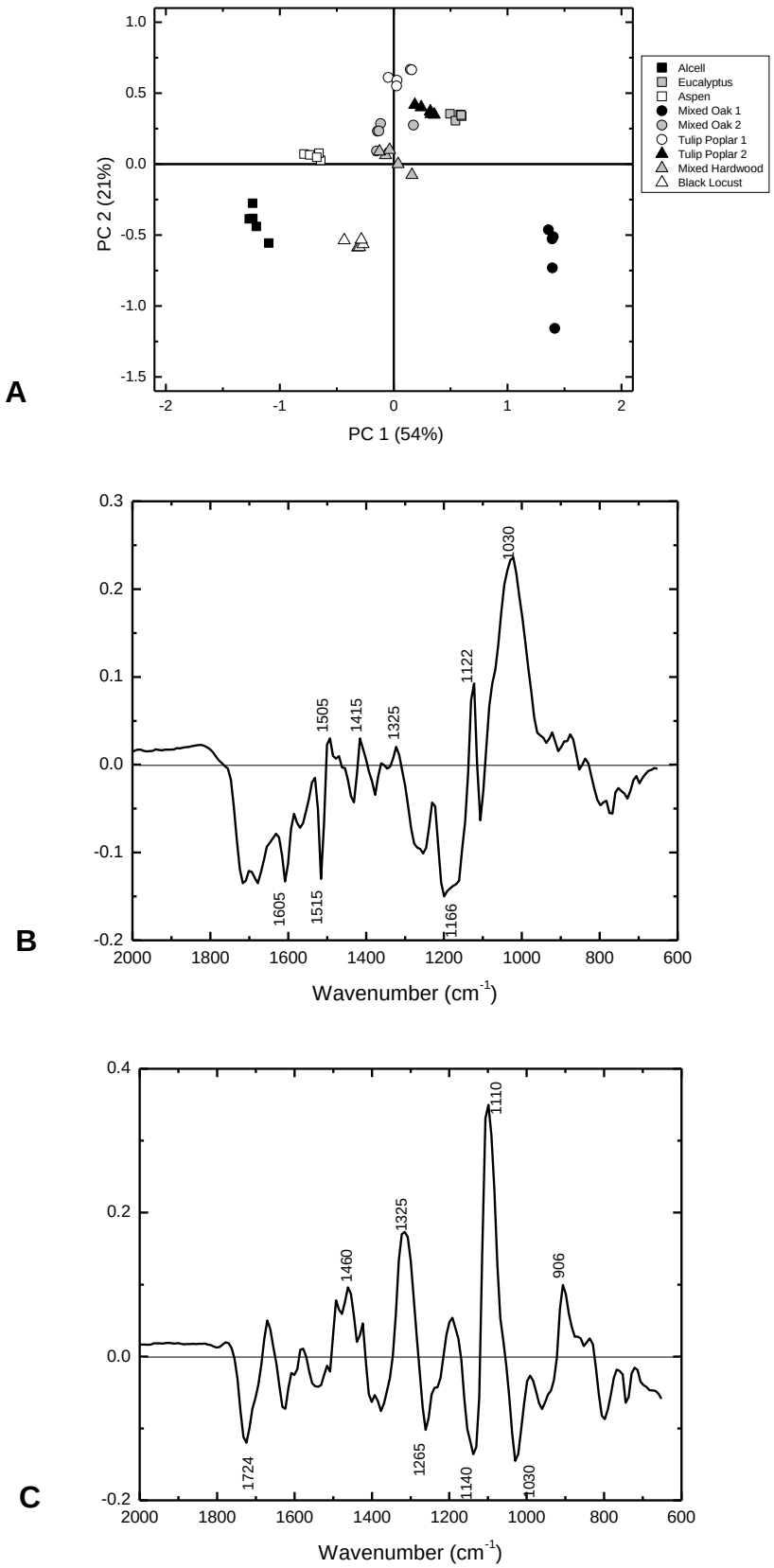

Fig. 3. (A) PC1 and PC2 Scores, (B) loading of PC1, and (C) loading of PC2 for selected hardwood lignins

The largest peaks are indicative of the key variations in structure between the different hardwood lignins. These variations come from the presence of S units as indicated by the peak at 1110 cm^{-1}, from the C-H bending of the G ring units as represented at 1140 cm^{-1}, and from the C-O deformation in the primary alcohols as represented at 1030 cm^{-1} (Faix 1991; Schultz and Glasser 1986; Popescu *et al.* 2007). This indicates that the concentrations of G rings and S rings as well as the presence of alcohol groups are key differences that separate the mixed hardwood lignins from the Alcell, black locust, aspen, tulip poplar, and eucalyptus lignins. As stated previously, this is also a key structural difference between the hardwood, softwood, and grass lignins.

Thermal Spectra Regression Analysis

Using the glass transition temperatures as well as the FT-IR spectra for all the lignin samples, a PLS regression was performed with the Unscrambler software. PLS provides a model for the relationship between a set of predictor variables and a set of response variables (Martens and Naes 1989). In this analysis, all but one sample was used as the predictor variable to create a calibration model. The remaining sample was used as a response variable for validation of the model. This approach ensured that the developed model was not over-predicted. A strong correlation (r = 0.96; RMSEC = 6.9°C) was obtained between the FTIR spectra and the T_g (Fig. 4A), indicating a relationship between the chemical fingerprint of lignin and its corresponding morphological structure. From Fig. 4A, the T_g of various hardwoods (*i.e.*, aspen and mixed hardwoods) spans the entire range of observations, demonstrating that biomass type does not determine T_g. (B)Figure 4B indicates the bands that represent the structural components of the lignin samples that have the greatest impact on the prediction of the glass transition temperature. The main bands are as follows: 1716 cm^{-1}, the non-conjugated carbonyls; 1670 cm^{-1}, the conjugated carbonyls; 1585 cm^{-1}, the aromatic ring for GS lignin; 1505 cm^{-1}, the aromatic GS ring; 1265 cm^{-1}, the C-O stretching of the G ring; 1110 cm^{-1}, the aromatic C-H deformation of S units; and 1030 cm^{-1}, the C-O deformation in the primary alcohols (Faix 1991; Schultz and Glasser 1986; Popescu *et al.* 2007). The following peaks are not part of the lignin spectra: 1370 cm^{-1} and 1000 cm^{-1}, from hemicelluloses (Xiao *et al.* 2001 and Sun *et al.* 2000). This indicates that there are residual polysaccharides present in the lignin samples that affect the T_g values of the lignin samples.

The strong peaks associated with the lignin spectra in Fig. 4B indicate that the carbonyls, the monomers of the lignin, especially for S ring units, as well as the primary alcohols and residual polysaccharides, have the greatest impact on the T_g. Results were obtained from the DSC analysis in which hardwood lignins with more S units spanned the whole breadth of the observed T_g values when compared to the softwood and grass lignins (Kubo and Kadla 2004). This could indicate that the concentration of the S rings within the lignin samples has an impact on the T_g values in a manner related to feedstock, but the processing conditions and purity could also play the largest role.

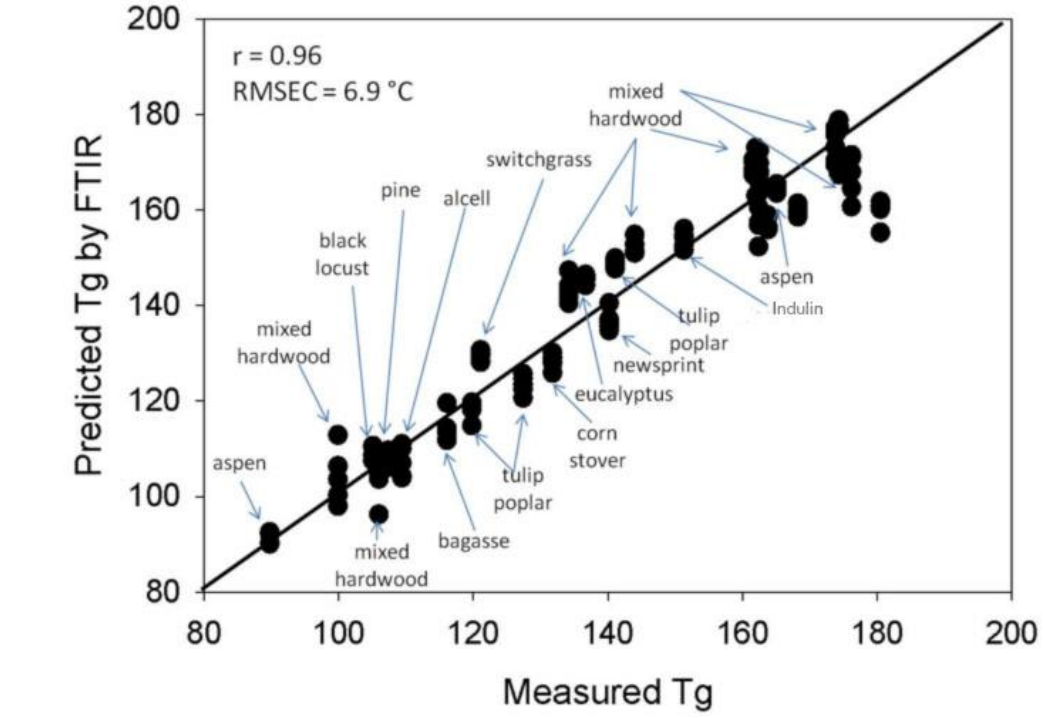

(A)

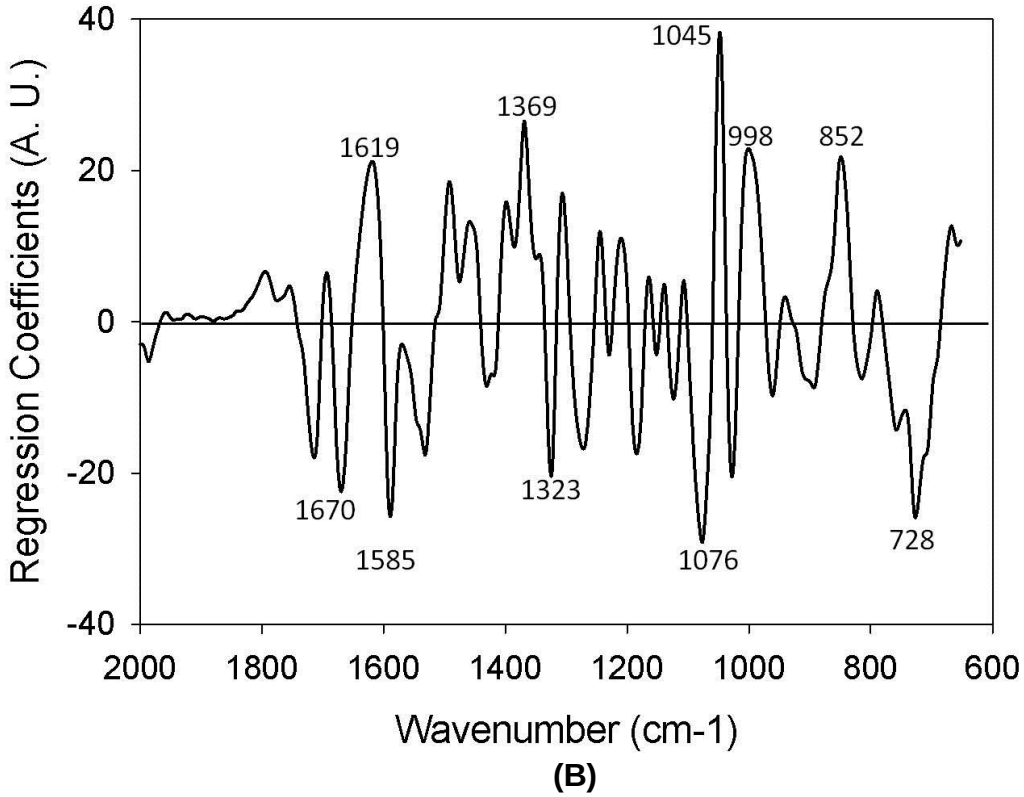

(B)

Fig. 4. (A) PLS analysis for all lignins and (B) regression coefficients

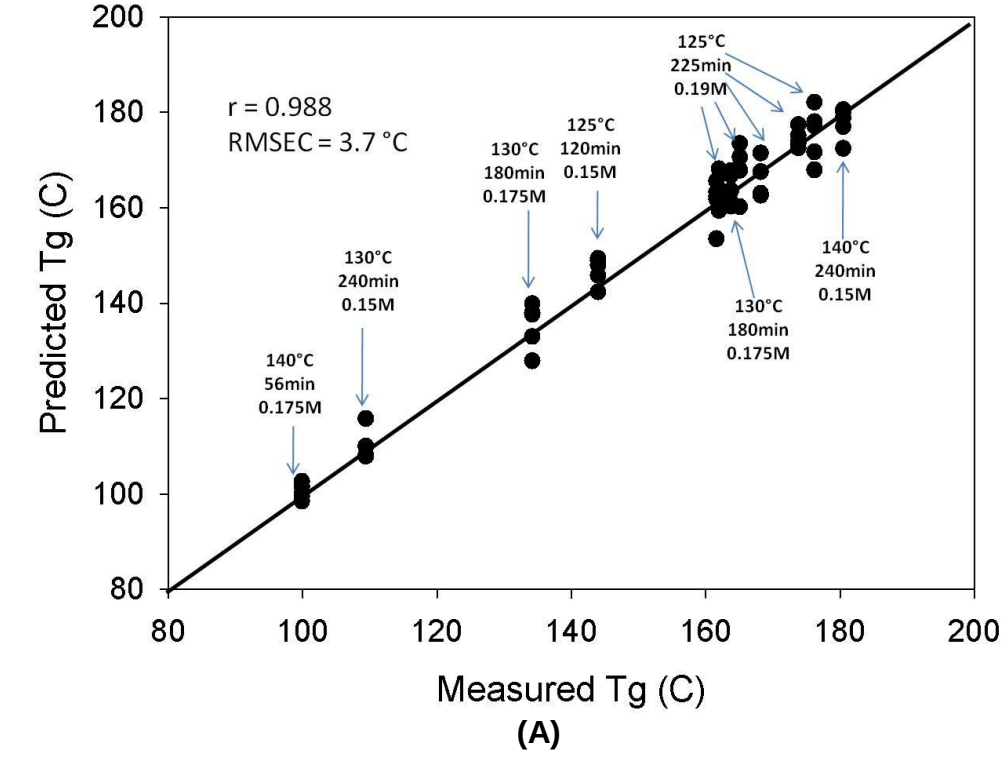

(A)

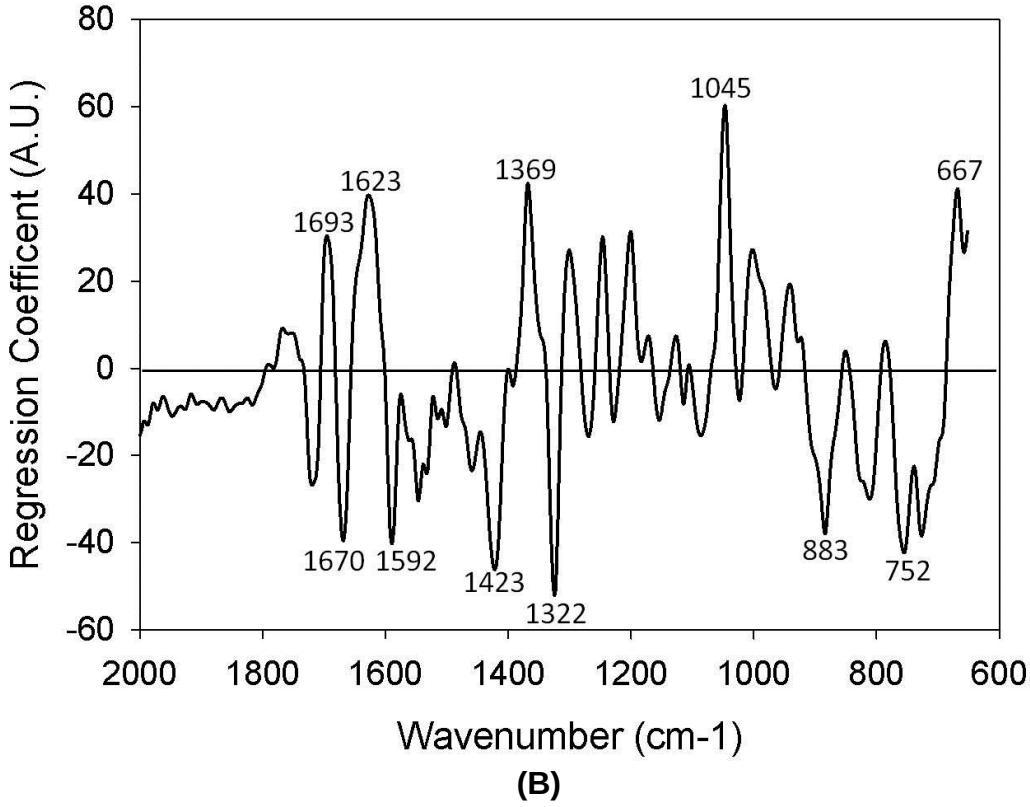

(B)

Fig. 5. (A) PLS analysis of mixed hardwood biomass for various processing conditions and (B) the regression coefficients

A subset of the lignins being studied was chosen in order to investigate the impact that processing conditions had on T_g for a single biomass type. Mixed hardwoods were chosen, as they displayed a wide T_g range and had been subjected to a range of processing conditions. A PLS analysis was performed on this feedstock and a very strong correlation (r = 0.988; RMSEC = 3.7°C) was obtained between the FTIR spectra model of T_g and the observed T_g (Fig. 5A). No readily discernable trend of correlation between processing condition and T_g was observed, yet the tendency appeared to be that longer processing times and higher acid concentrations produced a more condensed, higher T_g lignin. A more thorough understanding of the kinetics of the organosolv process is warranted in order to obtain a lignin with the desired thermal properties.

As previously observed, the 1045 cm^{-1} peak related to primary alcohols played an important role in T_g of the lignin (Fig. 5B). Also apparent was that there was less influence on the T_g in the mixed hardwoods from G units, as there was an absence of a distinct peak at 1268 cm^{-1}, but there is a clear peak at 1322 cm^{-1} that shows a strong influence from S units. Also, an influence from carbonyls (1693 and 1670 cm^{-1}) indicates the influence of the processing on the increased oxidation of the lignin and the resulting higher T_g. Furthermore, there was less influence of residual polysaccharides when softwoods and grasses were included in the analysis.

CONCLUSIONS

Using FT-IR spectral analysis coupled with statistical PCA revealed that there were significant differences in the structure of the lignin that existed particularly between the hardwood, softwood, and grass lignins. The PCA revealed that the hardwood lignin's S and G rings, as well as the presence of alcohols and ethers, are the key differences that separate hardwood lignins from other species. Ester groups and variations in the G ring are mainly what differentiate the softwood lignins from the grass lignins. The PCA of the hardwoods revealed little influence from residual polysaccharides but greater influence from the concentration of G units, ether linkages, carbonyls, and primary alcohols. The PCA did not reveal the influence of processing effects on hardwood lignin species.

The PLS regression revealed that T_g is greatly affected by the variations in structural differences of the lignins. The main structures that alter the thermal properties of the lignin are the concentrations of S ring units, which are a key structural difference between hardwoods, softwoods, and grass lignins, as is the concentration of primary alcohols. Nevertheless, the time and conditions of the extraction process tended to have a larger influence on T_g than did the biomass source. The starting biomass would also certainly affect the kinetics of this trend, and this warrants a more complete investigation. Thermal properties were also affected by the residual polysaccharides remaining from the organosolv process, but not to the same degree as observed from the S ring units. Species tends to have an effect on the amount of impurities left after fractionation. In other words, the grasses and possibly softwoods possessed a greater abundance of residual polysaccharides than was observed in the hardwoods. A more thorough understanding of the impact of processing conditions and lignin kinetics during the fractionation process is needed. Understanding the differences, as well as the similarities, resulting from the chemical structures and the physical properties in this new group of lignins is vital in determining how these lignins can be fully implemented as new products.

ACKNOWLEDGEMENTS

Financial support for this work was provided by the United States Department of Agriculture Biomass Research and Development Initiative agreement #67-3A75-5-22. Thermal analysis was conducted at the Center for Nanophase Materials Science at ORNL under user proposal CNMS2009-079.

REFERENCES CITED

Bozell, J. J., Black, S. K., Myers, M. Cahill, D., and Miller, W. P. (2011a). "Solvent fractionation of renewable woody feedstocks: Organosolv generation of biorefinery process streams for the production of biobased chemicals," *Biomass Bioenergy* 35, 4197-4208

Bozell, J. J., O'Lenick, C. J., and Warwick, S. (2011b). "Biomass fractionation for the biorefinery: Heteronuclear multiple quantum coherence – Nuclear magnetic resonance investigation of lignin isolated from solvent fractionation of switchgrass," *Journal of Agricultural and Food Chemistry* 59, 9232-9242.

El Hage, R., Brosse, N., Sannigrahi, P., and Ragauskas, A. (2010). "Effects of process severity on the chemical structure of *Miscanthus* ethanol organosolv lignin," *Polym Degradation Stability* 95, 997-1003.

Faix, O. (1991). "Classification of lignin from different botanical origins by FT-IR spectroscopy," *Holzforschung* 45, 21-27.

Feldman, D., Banu, D., Campanelly, J., and Zhu, H., (2001). "Blends of vinylic copolymer with plasticized lignin: Thermal and mechanical properties," *J. Applied Polym Sci.* 81, 861-874.

Geladi, P. (2003). "Chemometrics in spectroscopy. Part 1. Classical chemometrics," *Spectrochimica Acta B*, 58, 767-782.

Glasser, W. G., and Jain, R. K. (1993). "Lignin derivatives. I. Alkanoates," *Holzforschung* 47, 225-233.

Hamelinck, C. N., van Hooijdonk, G., and Faaij, A. P. C. (2005). "Ethanol from lignocellulosic biomass: Techno-economic performance in short-, middle- and long-term," *Biomass Bioenergy* 28, 384-410.

Khan, M. A., and Ashraf, S. M. (2007). "Studies on thermal characterization of lignin: Substituted phenol formaldehyde resin as wood adhesives," *J. Thermal Analysis and Calorimetry* 89, 993-1000.

Kirk, T. K., and Chang, H. M. (1981). "Potential applications of bio-ligninolytic systems," *Enzyme Microbial Technology* 3(3), 189-196.

Kubo, S., and Kadla, J. F. (2004). "Poly(ethylene oxide)/organosolv lignin blends: Relationship between thermal properties, chemical structure, and blend behavior," *Macromolecules* 37, 6904-6911.

Lora, J. H., and Glasser, W. G. (2002). "Recent industrial applications of lignin: A sustainable alternative to nonrenewable materials," *J. Polymers Environment* 10(1), 39-48.

Martens, H., and Naes, T. (1989). *Multivariate Calibration*, John Wiley and Sons. New York.

Popescu, C. M., Singurel, G., Vasile, C., Argyropoulos, D. S., and Willfor, S. (2007). "Spectral characterization of eucalyptus wood," *Applied Spectroscopy* 61(11), 1168-1177.

Schultz, T. P., and Glasser, W. G. (1986). "Quantitative Structural Analysis of Lignin by Diffuse Reflectance Fourier Transform Infrared Spectrometry," *Holzforschung* 40, 37-44.

Stewart, D. (2008). "Lignin as a base material for materials applications: Chemistry, application and economics," *Industrial Crops Products* 27, 202-207.

Sun, R. C., Tomkinson, J., Ma, P. L., and Liang, S. F. (2000). "Comparative study of hemicelluloses from rice straw by alkali and hydrogen peroxide treatments," *Carbohydrate Polymers* 42, 111-122.

Tejado, A., Peña, C., Labidi, J., Echeverria, J. M., and Mondragon, I. (2007). "Physico-chemical characterization of lignins from different sources for use in phenol–formaldehyde resin synthesis," *Bioresource Technology* 98, 1655-1663.

U.S. Department of Energy. (2011). *U.S. Billion-Ton Update: Biomass Supply for a Bioenergy and Bioproducts Industry.* R. D. Perlack and B. J. Stokes (Leads), ORNL/TM-2011/224. Oak Ridge National Laboratory, Oak Ridge, TN. 227p.

Xiao, B., Sun, X. F., and Sun, R. C. (2001). "Chemical, structural, and thermal characterizations of alkali-soluble lignins and hemicelluloses, and cellulose from maize stems, rye straw, and rice straw," *Polym Degradation Stability* 74, 307-319.

Article submitted: June 4, 2012; Peer review completed: February 2, 2013; Revised version received and accepted: April 15, 2013; Published: April 17, 2013.